Tunnel Engineering for Modulating The Substrate Preference in Decarbonylase P450BsβHI

Shuaiqi Meng
Beijing Bioprocess Key Laboratory, Beijing University of Chemical Technology, Beijing, 100029, PR China. Institute of Biotechnology, RWTH Aachen University, Worringerweg 3, Aachen 52074, Germany

Ruipeng An
Beijing Bioprocess Key Laboratory, Beijing University of Chemical Technology, Beijing, 100029, PR China

Zhongyu Li
Beijing Bioprocess Key Laboratory, Beijing University of Chemical Technology, Beijing, 100029, PR China

Ulrich Schwaneberg
Institute of Biotechnology, RWTH Aachen University, Worringerweg 3, Aachen 52074, Germany. DWI-Leibniz Institute for Interactive Materials, Forckenbeckstraße 50, Aachen 52074, Germany

Yu Ji
Institute of Biotechnology, RWTH Aachen University, Worringerweg 3, Aachen 52074, Germany

Mehdi D. Davari
Institute of Biotechnology, RWTH Aachen University, Worringerweg 3, Aachen 52074, Germany

Wang Fang
Beijing Bioprocess Key Laboratory, Beijing University of Chemical Technology, Beijing, 100029, PR China

Meng Wang
Beijing Bioprocess Key Laboratory, Beijing University of Chemical Technology, Beijing, 100029, PR China

Meng Qin
Beijing Bioprocess Key Laboratory, Beijing University of Chemical Technology, Beijing, 100029, PR China

Kaili Nie
Beijing Bioprocess Key Laboratory, Beijing University of Chemical Technology, Beijing, 100029, PR China

Luo Liu (liuluo@mail.buct.edu.cn)
Beijing University of Chemical Technology https://orcid.org/0000-0002-3542-8213

Research

Keywords: Tunnel engineering, Substrate Preference, P450 decarbonylase, α-Alkene biosynthesis, Rational design

Posted Date: December 23rd, 2020

DOI: https://doi.org/10.21203/rs.3.rs-132813/v1

Version of Record: A version of this preprint was published at Bioresources and Bioprocessing on April 3rd, 2021. See the published version at https://doi.org/10.1186/s40643-021-00379-1.

Abstract

An active site normally locates inside of enzymes, substrates should go through the tunnel to access the active site. Tunnel engineering is a powerful strategy for refining the catalytic properties of enzymes. Here, $P450_{Bs\beta}$HI (Q85H/ V170I) derived from hydroxylase $P450_{Bs\beta}$ from *Bacillus subtilis* was chosen as study model, which is reported as a potential decarbonylase. However, this enzyme showed low decarboxylase activity towards long-chain fatty acids. Here, a tunnel engineering campaign was performed for modulating the substrate preference and improving the decarbonylase activity of $P450_{Bs\beta}$HI. The finally obtained BsβHI-F79A variant had a 15.2-fold improved conversion for palmitic acid; BsβHI-F173V variant had a 3.9-fold improved conversion for pentadecanoic acid. The study demonstrates how the substrate preference can be modulated by tunnel engineering strategy.

1. Introduction

Enzymes are able to catalyze many specific reactions and are widely used in practical application. Previously, the enzyme functions were limited around their natural use; nowadays, the enzymes could be developed by engineering their activity and selectivity for meeting human demands (Bornscheuer et al., 2012; Damborsky and Brezovsky, 2014). Two common engineering strategies are the directed evolution based on Darwinian theory and rational design based on the structure-function relationship (Bornscheuer and Pohl, 2001). Rational design often focused on the substrate binding pocket which directly affluence the enzymatic process (Bornscheuer and Pohl, 2001). However, the experiences of directed evolution told us the residues outside the active site also influence the enzyme properties (Kress et al., 2018). Researching on those “non-hotspot” rather than typical active site may be beneficial for expanding the understanding of proteins.

The urgent problem now confronting us is how to obtain the important “non-hotspot” domains beyond the enzyme active site. Tunnel engineering may be one of the answers. Enzymes spanning all of the six classes are found the exist of the tunnels (Kingsley and Lill, 2015). It was reported that more than 64% enzymes annotated in Catalytic Site Atlas library have the buried active site with the tunnels connecting the enzyme binding pocket and the environment (Pravda et al., 2014). The tunnels could support the transport of solvent, product and solvent between the enzyme active site and bulk solvent, which play important role in enzymatic reaction (Kokkonen et al., 2019; Zhou and McCammon, 2010). The behavior of substrate on the tunnels to the active site could affect the activity, stability and substrate selectivity (Kingsley and Lill, 2015; Lu et al., 2019; Yu et al., 2013). A typical example might be that the R47 and Y51 residues, two polar amino acids located at the end of access tunnel of P450 BM3, could regulate the entry of substrate, water and co-solvents (Whitehouse et al., 2012). Cheng et al. found that a single position located on the access tunnel of nitrile hydratase could invert the regio-selectivity towards aliphatic α,ω-dinitriles (Cheng et al., 2016). Tunnel engineering is becoming a promising strategy to optimize the enzyme property. Several scientists have developed many algorithms for determination of enzymatic tunnels, such as CAVER (Kozlikova et al., 2014), MOLE (Sehnal et al., 2013), AQUA-DUCT (Magdziarz et al., 2017) and CCCPP (Benkaidali et al., 2014). However, compared with the prediction of tunnels, only a

few experimental tunnel engineering examples were reported (Kress et al., 2018). Here, we aim to develop the application of tunnel engineering for modulating the substrate preference.

α-alkenes are multifunctional compounds that perform an important industrial value and an extraordinary economic importance due to their flexible and active chemical performance. Particularly, long-chain α-alkenes can be used in the synthesis of high-value biofuel, lubrication and surfactant (Lee et al., 2008). However, α-alkenes mostly come from non-renewable petroleum cracking (Dutta et al., 2014). Energy-intensive process and harsh reaction conditions prompted researchers to focus on enzymatic synthetic strategy of α-alkenes (Schirmer et al., 2010). To date, three biotransformation strategies that convert fatty acids or its derivative to alkene were reported (Yi et al., 2014). A three-gene cluster from *Micrococcus luteus* represented a production of long-chain alkenes from a head-to-head condensation of fatty acids (Beller et al., 2010); a type I polyketide synthases from *Synechococcus* sp. was involved in a production of medium-chain α-alkenes via an elongation decarboxylation mechanism (Mendez-Perez et al., 2011); and some members from cytochrome P450 family are able to decarboxylate fatty acids and produce α-alkenes directly (Grant et al., 2015; Hsieh and Makris, 2016). Among those pathways, the decarboxylic reaction catalyzed by P450 is the simplest strategy. Free fatty acids could be used as substrate directly, which represent potential of producing α-alkenes on a large-scale based in engineered cell factory.

Representative P450 decarboxylases belong to CYP152 subfamily, such as $P450_{Bs\beta}$ (CYP152A1) from *Bacillus subtilis* (Matsunaga et al., 1999), $P450_{Sp\alpha}$ (CYP152B1) from *Sphingomonas paucimobilis* (Matsunaga et al., 2000), and $P450_{oleT}$ (CYP152L1) from *Jeotgalicoccus sp.* (Yi et al., 2014). As the first member of CYP152 subfamily, $P450_{Bs\beta}$ was the research hotspot since it was discovered by Isamu *et al.* in 1999. However, wild-type $P450_{Bs\beta}$ showed higher hydroxylation activity rather than decarboxylation activity (Matsunaga, et al., 1999). In contrast, $P450_{oleT}$ presented prominent decarboxylation property, which is able to convert medium- or long-chain fatty acids to corresponding carboxylic acids (Rude et al., 2011). Interestingly, some $P450_{Bs\beta}$ variants also exhibited satisfactory decarboxylation ability. Xu *et al.* reported a $P450_{Bs\beta}$HI variant (Q85H/V170I) which displayed enhanced decarboxylation activity towards medium- or long-chain fatty acids (Xu et al., 2017). However, the yield of α-alkenes drops sharply as the length of the carbon chain of the substrate increases, which is the main limitation of the use of $P450_{Bs\beta}$HI for long chain α-alkenes synthesis.

In the present work, we systematically analyzed the access tunnels in decarbonylase $P450_{Bs\beta}$HI. In order to improve the substrate preference of $P450_{Bs\beta}$HI to long chain fatty acids, two residues related to the access tunnels diameter were identified and mutated. In addition, the substrate selection mechanism controlled by tunnels of $P450_{Bs\beta}$HI was briefly discussed.

2. Experimental

2.1. Strain, plasmid and chemicals

Escherichia. coli strain BL21(DE3) cells (used for gene expression) and TOP10 cells (used for molecular cloning) were purchased from TransGen Ltd. (China) The gene BsβHI-wt (NCBI Reference Sequence: WP_119898938.1) was synthesized by Inovogen Ltd. (China). Fast Mutagenesis kit was from Vazyme Biotech Co., Ltd (China). Plasmid extraction kits and gel extraction kits were obtained from Omega Bio-tek (USA). Capric acid, lauric acid, myristic acid, stearic acid, undecene and tridecene were purchased from BioRo Yee Ltd. (China). All chemicals used were of analytical grade.

2.2. Molecular modeling and simulation

The structure model of $P450_{Bs\beta}HI$ was constructed by PyMoL Molecular Graphics System (version 2.3.3) based using the crystal structure of $P450_{Bs\beta}$ from *Bacillus subtilis* (PDB code: 1IZO with the resolution in 2.10 Å) as template (Lee et al., 2003). Molecular dynamics simulation was carried out in YASARA (version 17.8.15) using the built-in MD macro “md_run.mrc” with the AMBER03 force field (Hess et al., 2008). Structure were solvated into a 12 Å cube simulation cell of water molecules. The box was filled with 3857 water molecules. The simulations of the protein-water system was performed at 303 K, pH value of 8.0. Na^+ and Cl^- were used to neutralize the systems. In all simulations, constant pressure periodic boundary conditions were used for 5 ns MD production. The simulation snapshots were capture every 100 ps from 2.5 ns to 5 ns (after RMSD stabilizes).

2.3. Tunnel analysis

Tunnel analyzed by MOLEonline (Pravda et al., 2018) with following parameters: Interior treshold 1.1 Å, Bottleneck Tolerance 3 Å, bottleneck radius 1.2 Å. Probe Radius 5 Å, Surface CoverRadius 10 Å. The starting point was the heme cofactor. Water molecules were not considered in channel analyses.

Tunnels analyzed by Caver Analyst 2.0 BETA (Jurcik et al., 2018) with following procedures: After the MD simulation, 25 snapshots were introduced to Caver Analyst 2.0 BETA. Tunnel calculations were performed with the analytical parameters as follow: probe radius of 1.4 Å, shell depth of 4 Å, shell radius of 3 Å, clustering threshold of 3.5, and the starting point of surrounding the residues of R242, P243, and heme. After the tunnel calculations, the influence of the tunnel by related residues was extracted from the function of tunnel statistics and residue graph. Finally, amino acid residues with significant influence on the tunnel bottleneck were selected for further mutagenesis experiments.

2.4. Relative folding free energies (ΔΔGfold) analysis

The ΔΔGfold values were calculated using FoldX employing the YASARA plugin (version 19.12.4). The structure model of $P450_{Bs\beta}HI$ and its variants were constructed by PyMoL Molecular Graphics System (version 2.3.3) based using the crystal structure of $P450_{Bs\beta}$ from *Bacillus subtilis* (PDB code: 1IZO with the resolution in 2.10 Å) as template. The initial structure of $P450_{Bs\beta}HI$ was constructed by the Automated Modeling Tool of Swiss Model Web Service (http://swissmodel.expasy.org/) using the crystal structure of P450Bsβ from Bacillus subtilis (PDB code: 1IZO with the resolution in 2.10 Å) as template. FoldX parameters was temperature 298 K, pH 8, and 0.05 M ionic strength.

2.5. Site-specific mutagenesis

The $P450_{Bs\beta}$HI gene was inserted into plasmid pET22b(+) between the NdeI and HindIII restriction nuclease sites, with the His-tag encoding sequence at N-terminal. All of the variants were done by Fast Mutagenesis kit.

The variants with single mutation used $P450_{Bs\beta}$HI as template, in which F79 and F173 site was dividually replaced with relatively small amino acids, including glycine, valine, alanine, serine, isoleucine, threonine, cysteine, leucine, and proline. Variants with double mutations used BsβHI-F173V variant as template.

2.6. Heterologous expression and purification

$P450_{Bs\beta}$HI and its variants were transferred to *E. coli* BL21(DE3) for expression. Recombinant *E. coli* BL21 (DE3) cells were grown in LB medium (5 g/L yeast extract, 10 g/L tryptone, and 5 g/L NaCl) supplemented with ampicillin (100 μg/ml) at 37 ℃ until the OD600 reached about 0.6. All of genes were induced by the addition of 0.1 mM of isopropyl-β-d-thiogalactopyranoside (IPTG) at 18℃ for 12 h. Then the cells were harvested and ultrasonic broken. Cell-free extractions were used for purification.

Enzymes were purified by His-tag affinity chromatography. Cell-free extractions was loaded onto a Ni-NTA column and equilibrated by Lysis buffer (50 mM of Tris-HCl, 10 mM of imidazole and 300 mM of NaCl, pH 7.8). Then the protein was sequential eluted by Wash buffer (50 mM of Tris-HCl, 30 mM of Iimidazole and 300 mM of NaCl, pH 7.8) and Elution buffer (50 mM of Tris-HCl, 300 mM of imidazole and 300 mM of NaCl, pH 7.8). Eluates were concentrated with an ultrafiltration (Millipore, Germany). The concentrations of purified proteins were determined by BCA kit (Solarbio, China).

2.7. Enzymatic assay

The bio-catalytic system contained 10 μM $P450_{Bs\beta}$HI enzyme (or its variants), 500 μM fatty acid substrate (from a 100 mM stock solution in ethanol) and 1 mM H_2O_2 in a final volume of 1 mL of 100 mM potassium phosphate buffer (pH = 8.0). The reaction was carried out at 30℃ for 2 h, then was quenched by additional 50 μL of 6 M HCl. The mixture was extracted by 800 μL hexane. Following extraction, the products were analyzed by gas chromatography-mass spectrometry (GC-MS-QP2020, Shimadzu, Japan) equipped with a Sh-Rxi-5Sil-Ms column (Shimadzu, Japan) using helium as carrier gas. The oven temperature was controlled initially at 50℃ for 2 min, then increased at the rate of 10℃ min^{-1} to 280℃, and held for 10 min. The injecting temperature was 280℃. The peaks were identified by comparison of retention time and ion spectra with authentic references.

3. Results And Discussion

The result and discussion part is divided into three parts. In the first part, the $P450_{Bs\beta}$HI access tunnels were analyzed and two amino acids were identified as beneficial key residues. In the second part, the variants based on the two key residues were characterized with lauric acid substrate then 5 best variants were selected. In the third part, the substrate preference of selected $P450_{Bs\beta}$HI variants was investigated.

3.1. $P450_{Bs\beta}HI$ access tunnel analysis and hot spots identification

Access tunnels is responsible for ligand transportation between active site and solvent environment in enzymes with buried active site (Kokkonen et al., 2019). Using MOLEonline serve (L. Pravda et al., 2018), two access tunnels were found in $P450_{Bs\beta}HI$ (Fig. 1A, 1B **and** Table 1). The tunnels showed typical cytochrome features. The F and G helix define the most common tunnels among cytochrome P450s (Cojocaru et al., 2007). The peripheral flexible F-G loop can control the tunnel topology then influence substrate recognition. Representative tunnel in $P450_{Bs\beta}HI$ is Tunnel 1, which goes through the A helix, B' helix, B-B' loop B'-C loop, and F-G loop. Tunnel 1 consists of a large number of non-polar residues, which facilitates the access of hydrophobic substrates (**Table S1**). Tunnel 2 threads through B-B' loop and B'-C loop, which is also common among P450s. Compared with Tunnel 1, Tunnel 2 is shows higher polarity and contains a hydrophilic area near the surface of $P450_{Bs\beta}HI$ (Fig. 1C **and** Table 1**)**. In addition to participating in substrate transport, this tunnel may be also involved the controlling water diffusion.

Table 1
The properties of identified access tunnels in $P450_{Bs\beta}HI$. The access tunnel analysis was carried out with MOLEonline.

Tunnel	Length (Å)	Bottleneck radius (Å)	Polarity*
Tunnel 1	29	1.4	4.06
Tunnel 2	37	1.2	8.48

* Polarity is calculated as an average of amino acid polarities assigned according to the method of Zimmerman et al. (Zimmerman, Eliezer, & Simha, 1968) Polarity ranges from completely nonpolar amino acids (ALA, GLY = 0.00) through polar residues (e.g. SER = 1.67) towards charged residues (GLU = 49.90, ARG = 52.00).

In order to find potentially important residues, we set four criterions: 1.) Located in the tunnel bottleneck area; 2) being high influential among the entire tunnel; 3) Located in the loop area; 4) being not completely conserved in its homologous cytochromes. Caver Analyst 2.0 software was chosen for analyzing the residues influence, which provide an opportunity to explore the portion of the tunnel influenced by a particular amino acid (Jurcik et al., 2018). We analyzed the tunnel properties and bottleneck residues influence over 5 ns (Fig. 2). The results indicate that residues of F173 and V74 have high impact on Tunnel 1, and H85 and F79 are the main bottleneck residues in access Tunnel 2. Among high impact residues, H85 is the core residues for $P450_{Bs\beta}HI$ decarboxylation activity (Xu et al., 2017), V74 is located in the middle of B' helix, while the two phenylalanine, F79 and F173, are non-conservative (**Figure S1**) and located in the B'-C loop and F-G loop, respectively. Given that, F79 and F173 residues were chosen for further analysis to optimize the enzymatic property while avoid ruining tunnel architecture.

Theoretically, the transport ability of substrates between enzyme active site and solvent environment could be adjusted by gates located at the access tunnels (Gora et al., 2013). Aromatic amino acids in access tunnels bottleneck are often participated in the control of the putative gates (Pavlova et al., 2009). As show in Fig. 2, the huge aromatic side chains of F79 and F173 were involved in the tunnel bottleneck regions. Here, the two phenylalanine residues F79 and F173 are presumed to be the “gatekeeper”, i.e. control the access of substrate from solvent environment to $P450_{Bs\beta}HI$ active site. In addition, the F79 and F173 are also deemed to stabilize the fatty acid substrates via hydrophobic interactions (Lee et al., 2003). Based on the critical location of the two residues, it is assumed the large phenyl side chain of phenylalanine maintains substrate stability, but hinders the entry of long-chain fatty acid substrates. A more flexible substrate entrance may benefit to increase enzyme activity towards long-chain fatty acids substrate. To test the hypothesis, the F79 and F173 residues were replaced by relatively small amino acid including cysteine, isoleucine, leucine, alanine, glycine valine, serine, threonine and proline, in mutagenesis experiments, respectively. The variants stability was evaluated by analysis of the relative free energy of folding ($\Delta\Delta G_{fold}$) (Cui et al., 2020) and no unstable substitution was found (**Figure S2**). Variants were heterologously expressed in *E. coil* BL21(DE3).

3.2. Decarbonylation activity of $P450_{Bs\beta}HI$ variants

As a hydrogen peroxide-dependent decarboxylase, $P450_{Bs\beta}HI$ relies on H_2O_2 as an electrons provider and oxygen supplier (Xu et al., 2017). To select promising variants of $P450_{Bs\beta}HI$, we examined the enzyme activity with the substrate of lauric acid using H_2O_2 as the sole co-factor. Decarboxylation efficiency was characterized by α-undecene yield. As shown in Fig. 3, 9 of 18 single-site variants showed improved yield of α-undecene. Particularly, BsβHI-F79A, BsbHI-F79S, BsβHI-F79T, BsβHI-F79V, and BsβHI-F173V exhibited more than 1.5 fold increase of α-undecene yield compared to $P450_{Bs\beta}HI$. The optimal variant BsβHI-F79T and BsβHI-F79V showed the 3.1-fold improvement of α-undecene yield. Then we focused on the alterations of identified tunnels in beneficial variants using MOLEonline serve (**Table S3**). The trends of decreased tunnel length and increased bottleneck radius were observed in the putative substrate tunnels (Tunnel 1) among variants, which is consistent with our previous assumptions. F79A variant showed the shortest substrate tunnel and the widest bottleneck radius, which were 2.8 Å decrease and 0.4 Å improvement, respectively. Interestingly, for both F79 or F173, we observed that the best decarboxylation performances were achieved by the valine substitution. The obvious feature of those two variants is the wider Tunnel 2. It is speculated that Tunnel 2 also undertakes the tunnel transfer task although this tunnel prefer polar water. Compared with Tunnel 1, Tunnel 2 has a longer length and a narrower bottleneck, which indicates that the Tunnel 2 may only serve as an auxiliary transportation for substrate. In short, the results indicated that the replacement of phenylalanine residue in positions 79 and 173 to relatively small amino acids (less bulky) had significant effect on the tunnels property and enzyme activity of $P450_{Bs\beta}HI$.

To further investigate the influence of substitution combination on the catalytic performance of $P450_{Bs\beta}HI$, we recombined the beneficial substitutions. Therefore, a series of double-site variants were constructed, which were BsβHI- F79A/F173V, BsβHI-F79S/F173V, BsβHI-F79T/F173V, and BsβHI-

F79V/F173V. However, all of the double-site variants show very low α-undecene production. One possibility is that the fatty acid substrates locate in the binding pocket lost the sufficient stability in the double site variants. The original F79 and F173 residues stabilize the substrate by hydrophobic interaction, so that substrate is structurally complementary to the $P450_{Bs\beta}HI$ active site. Although the lauric acid substrate is more accessible to the binding pocket after double-site variants, the lack of strong hydrophobic interaction with F79 and F173 residues resulted in flexible and instable binding of substrate around heme. Hence, the single-site variants of BsβHI-F79A, BsbHI-F79S, BsβHI-F79T, BsβHI-F79V, and BsβHI-F173V were chosen for further test.

3.3. Investigation of substrate preference in $P450_{Bs\beta}HI$ variants

Four additional fatty acids (capric acid, myristic acid, pentadecanoic acid, and palmitic acid) were investigated to probe the substrate profile of $P450_{Bs\beta}HI$ variants and explain whether the decarboxylation activity of $P450_{Bs\beta}HI$ variants are improved towards other medium- and long-chain fatty acids. In addition, given that the important industrial application of styrene, phenylpropionic acid was also added for testing. As shown in Fig. 4, the decarboxylation activities of BsβHI-F79T, BsβHI-F79V, and BsβHI-F173V are higher than $P450_{Bs\beta}HI$ with the capric acid as substrate. While toward long-chain fatty acids substrate, as a general trend, all candidates of $P450_{Bs\beta}HI$ variants exhibit higher catalytic efficiency than $P450_{Bs\beta}HI$. Intriguingly, optimal decarboxylation efficiency towards different substrates is exist in different variants. BsβHI-F173V possesses the highest activity towards myristic acid and pentadecanoic acid, while BsβHI-F79A is the best to palmitic acid. Both the two variants possessed broader access tunnels than the tunnels in $P450_{Bs\beta}HI$ (**Table S3**). We reasoned that this observation may stem from the compatibility between the substrate and access tunnels. Alanine has the smallest side chain, so it provided the F79A variant the widest substrate tunnel, which is able to accommodate relatively larger fatty acid substrate, like palmitic acid. Meanwhile, hydrophobic interaction provided by nonpolar alanine or valine also reduces substrate flexibility to fatty acids substrate, leading to higher stability of enzyme-substrate complex during the reaction cycle. In addition, only trace styrene was detected when used the phenylpropionic acid as substrate, probably due to the strong preference of $P450_{Bs\beta}HI$ towards fatty acid substrates (Xu et al., 2017).

4. Conclusions

Overall, an access tunnel engineering was carried out to understand the substrate preference as well as for improving the decarboxylation activity and of $P450_{Bs\beta}HI$. The structure indicates that two residues (F79 and F173) locate in the bottleneck of tunnels. A series of variants of $P450_{Bs\beta}HI$ were generated and investigated. Significantly improved decarboxylation activity was observed in BsβHI-F79A and BsβHI-F173V variants towards long-chain fatty acids. The results reveal that the appropriate reduction of the amino acid size at the gate of tunnels improves the enzymatic activity towards larger substrates, like long-chain fatty acids. Furthermore, our study shows that identifying and engineering key residues lining

the access tunnels may be a valuable and efficiency strategy for improving the performance of enzymes with buried active sites.

Declarations

Ethics approval and consent to participate

Not applicable

Consent for publication

Not applicable

Availability of data and materials

All data generated or analyzed during this study are included in this article and the supplementary information file.

Competing interests

The authors declare that they have no known competing financial interests or personal relationships that could have appeared to influence the work reported in this paper.

Funding

This study was funded by the National Natural Science Foundation of China (grant number 31961133017, 21978017, 21978020, 21861132017), the Fundamental Research Funds for the Central Universities XK1802-8. Shuaiqi Meng was supported by a Ph.D. scholarship from the China Scholarship Council (CSC No. 201906880011)

Authors' contributions

SQ-M performed the experiments and wrote this paper; RP-A and Prof. KL-N contributed to the calculation part; ZY-L analyzed the data; Prof. U-S, Dr. Y-J, Dr. MD-D helped to improve the paper; Prof. F-W, and Prof. M-Q and Dr. M-W were involved project administration, Prof. L-L designed the project and wrote the draft. All authors read and approved the final manuscript.

Acknowledgements

Not applicable

References

1. Beller, H. R., Goh, E. B., & Keasling, J. D. (2010). Genes involved in long-chain alkene biosynthesis in Micrococcus luteus. Appl Environ Microbiol, 76(4), 1212-1223.

2. Benkaidali, L., Andre, F., Maouche, B., Siregar, P., Benyettou, M., Maurel, F., et al. (2014). Computing cavities, channels, pores and pockets in proteins from non-spherical ligands models. Bioinformatics, 30(6), 792-800.
3. Bornscheuer, U. T., Huisman, G. W., Kazlauskas, R. J., Lutz, S., Moore, J. C., & Robins, K. (2012). Engineering the third wave of biocatalysis. Nature, 485(7397), 185-194.
4. Bornscheuer, U. T., & Pohl, M. (2001). Improved biocatalysts by directed evolution and rational protein design. Curr Opin Chem Biol 5(2), 137-143.
5. Cheng, Z., Cui, W., Liu, Z., Zhou, L., Wang, M., Kobayashi, M., et al. (2016). A switch in a substrate tunnel for directing regioselectivity of nitrile hydratases towards α,ω-dinitriles. Catal Sci Technol, 6(5), 1292-1296.
6. Cid, H., Bunster, M., Canales, M., & Gazitúa, F. (1992). Hydrophobicity and structural classes in proteins. Protein Eng Des Sel, 5(5), 373-375.
7. Cojocaru, V., Winn, P. J., & Wade, R. C. (2007). The ins and outs of cytochrome P450s. Biochim Biophys Acta, 1770(3), 390-401.
8. Cui, H., Cao, H., Cai, H., Jaeger, K. E., Davari, M. D., & Schwaneberg, U. (2020). Computer-Assisted Recombination (CompassR) Teaches us How to Recombine Beneficial Substitutions from Directed Evolution Campaigns. Chemistry, 26(3), 643-649.
9. Damborsky, J., & Brezovsky, J. (2014). Computational tools for designing and engineering enzymes. Curr Opin Chem Biol, 19, 8-16.
10. Dutta, K., Daverey, A., & Lin, J. G. (2014). Evolution retrospective for alternative fuels: first to fourth generation. Renew Energ, 69(3), 114-122.
11. Gora, A., Brezovsky, J., & Damborsky, J. (2013). Gates of enzymes. Chem Rev, 113(8), 5871-5923.
12. Grant, J. L., Hsieh, C. H., & Makris, T. M. (2015). Decarboxylation of fatty acids to terminal alkenes by cytochrome P450 compound I. J Am Chem Soc, 137(15), 4940-4943.
13. Hess, B., Kutzner, C., Van Der Spoel, D., & Lindahl, E. (2008). GROMACS 4: algorithms for highly efficient, load-balanced, and scalable molecular simulation. J Chem Theory Comput, 4(3), 435-447.
14. Hsieh, C. H., & Makris, T. M. (2016). Expanding the substrate scope and reactivity of cytochrome P450 OleT. Biochem Biophys Res Commun, 476(4), 462-466.
15. Jurcik, A., Bednar, D., Byska, J., Marques, S. M., Furmanova, K., Daniel, L., et al. (2018). CAVER Analyst 2.0: analysis and visualization of channels and tunnels in protein structures and molecular dynamics trajectories. Bioinformatics, 34(20), 3586-3588.
16. Kingsley, L. J., & Lill, M. A. (2015). Substrate tunnels in enzymes: structure-function relationships and computational methodology. Proteins, 83(4), 599-611.
17. Kokkonen, P., Bednar, D., Pinto, G., Prokop, Z., & Damborsky, J. (2019). Engineering enzyme access tunnels. Biotechnol Adv, 37(6), 107386.
18. Kozlikova, B., Sebestova, E., Sustr, V., Brezovsky, J., Strnad, O., Daniel, L., et al. (2014). CAVER Analyst 1.0: graphic tool for interactive visualization and analysis of tunnels and channels in protein

structures. Bioinformatics, 30(18), 2684-2685.

19. Kress, N., Halder, J. M., Rapp, L. R., & Hauer, B. (2018). Unlocked potential of dynamic elements in protein structures: channels and loops. Curr Opin Chem Biol, 47, 109-116.
20. Lee, D. S., Yamada, A., Sugimoto, H., Matsunaga, I., Ogura, H., Ichihara, K., et al. (2003). Substrate recognition and molecular mechanism of fatty acid hydroxylation by cytochrome P450 from Bacillus subtilis. Crystallographic, spectroscopic, and mutational studies. J Biol Chem, 278(11), 9761-9767.
21. Lee, S. K., Chou, H., Ham, T. S., Lee, T. S., & Keasling, J. D. (2008). Metabolic engineering of microorganisms for biofuels production: from bugs to synthetic biology to fuels. Curr Opin Biotechnol, 19(6), 556-563.
22. Lu, Z., Li, X., Zhang, R., Yi, L., Ma, Y., & Zhang, G. (2019). Tunnel engineering to accelerate product release for better biomass-degrading abilities in lignocellulolytic enzymes. Biotechnol Biofuels, 12, 275.
23. Magdziarz, T., Mitusinska, K., Goldowska, S., Pluciennik, A., Stolarczyk, M., Lugowska, M., et al. (2017). AQUA-DUCT: a ligands tracking tool. Bioinformatics, 33(13), 2045-2046.
24. Matsunaga, I., ., Ueda, A., ., Fujiwara, N., ., Sumimoto, T., ., & Ichihara, K., . (1999). Characterization of the ybdT gene product of Bacillus subtilis: novel fatty acid beta-hydroxylating cytochrome P450. Lipids, 34(8), 841.
25. Matsunaga, I., Sumimoto, T., Ueda, A., Kusunose, E., & Ichihara, K. (2000). Fatty acid-specific, regiospecific, and stereospecific hydroxylation by cytochrome P450 (CYP152B1) from Sphingomonas paucimobilis : Substrate structure required for α-hydroxylation. Lipids, 35(4), 365-371.
26. Mendez-Perez, D., Begemann, M. B., & Pfleger, B. F. (2011). Modular Synthase-Encoding Gene Involved in α-Olefin Biosynthesis in Synechococcus sp. Strain PCC 7002. Appl Environ Microbiol (No.12), 4264-4267.
27. Pavlova, M., Klvana, M., Prokop, Z., Chaloupkova, R., Banas, P., Otyepka, M., et al. (2009). Redesigning dehalogenase access tunnels as a strategy for degrading an anthropogenic substrate. Nat Chem Biol, 5(10), 727-733.
28. Pravda, L., Berka, K., Vařeková, R. S., Sehnal, D., Banáš, P., Laskowski, R. A., et al. (2014). Anatomy of enzyme channels. BMC bioinformatics, 15(1), 379.
29. Pravda, L., Sehnal, D., Tousek, D., Navratilova, V., Bazgier, V., Berka, K., et al. (2018). MOLEonline: a web-based tool for analyzing channels, tunnels and pores (2018 update). Nucleic Acids Res, 46(W1), W368-W373.
30. Rude, M. A., Baron, T. S., Shane, B., Murtaza, A., Cardayre, S. B., Del, & Andreas, S. (2011). Terminal olefin (1-alkene) biosynthesis by a novel p450 fatty acid decarboxylase from Jeotgalicoccus species. Applied & Environ Microbiol, 77(5), 1718.
31. Schirmer, A., Rude, M. A., Li, X., Popova, E., & Cardayre, S. B. d. (2010). Microbial Biosynthesis of Alkanes. Science(No.5991), 559-562.

32. Sehnal, D., Vařeková, R. S., Berka, K., Pravda, L., Navrátilová, V., Banáš, P., et al. (2013). MOLE 2.0: advanced approach for analysis of biomacromolecular channels. J Cheminformatics, 5(1), 39.
33. Whitehouse, C. J., Bell, S. G., & Wong, L. L. (2012). P450(BM3) (CYP102A1): connecting the dots. Chem Soc Rev, 41(3), 1218-1260.
34. Xu, H., Ning, L., Yang, W., Fang, B., Wang, C., Wang, Y., et al. (2017). In vitro oxidative decarboxylation of free fatty acids to terminal alkenes by two new P450 peroxygenases. Biotechnol Biofuels 10(1), 208.
35. Yi, L., Cong, W., Jinyong, Y., Wei, Z., Wenna, G., Xuefeng, L., et al. (2014). Hydrogen peroxide-independent production of α-alkenes by OleTJE P450 fatty acid decarboxylase. Biotechnology for Biofuels, 7(1), 28-28.
36. Yu, X., Cojocaru, V., & Wade, R. C. (2013). Conformational diversity and ligand tunnels of mammalian cytochrome P450s. Biotechnol Appl Biochem, 60(1), 134-145.
37. Zhou, H. X., & McCammon, J. A. (2010). The gates of ion channels and enzymes. Trends Biochem Sci, 35(3), 179-185.
38. Zimmerman, J., Eliezer, N., & Simha, R. (1968). The characterization of amino acid sequences in proteins by statistical methods. J. Theor. Biol, 21(2), 170-201.

Figures

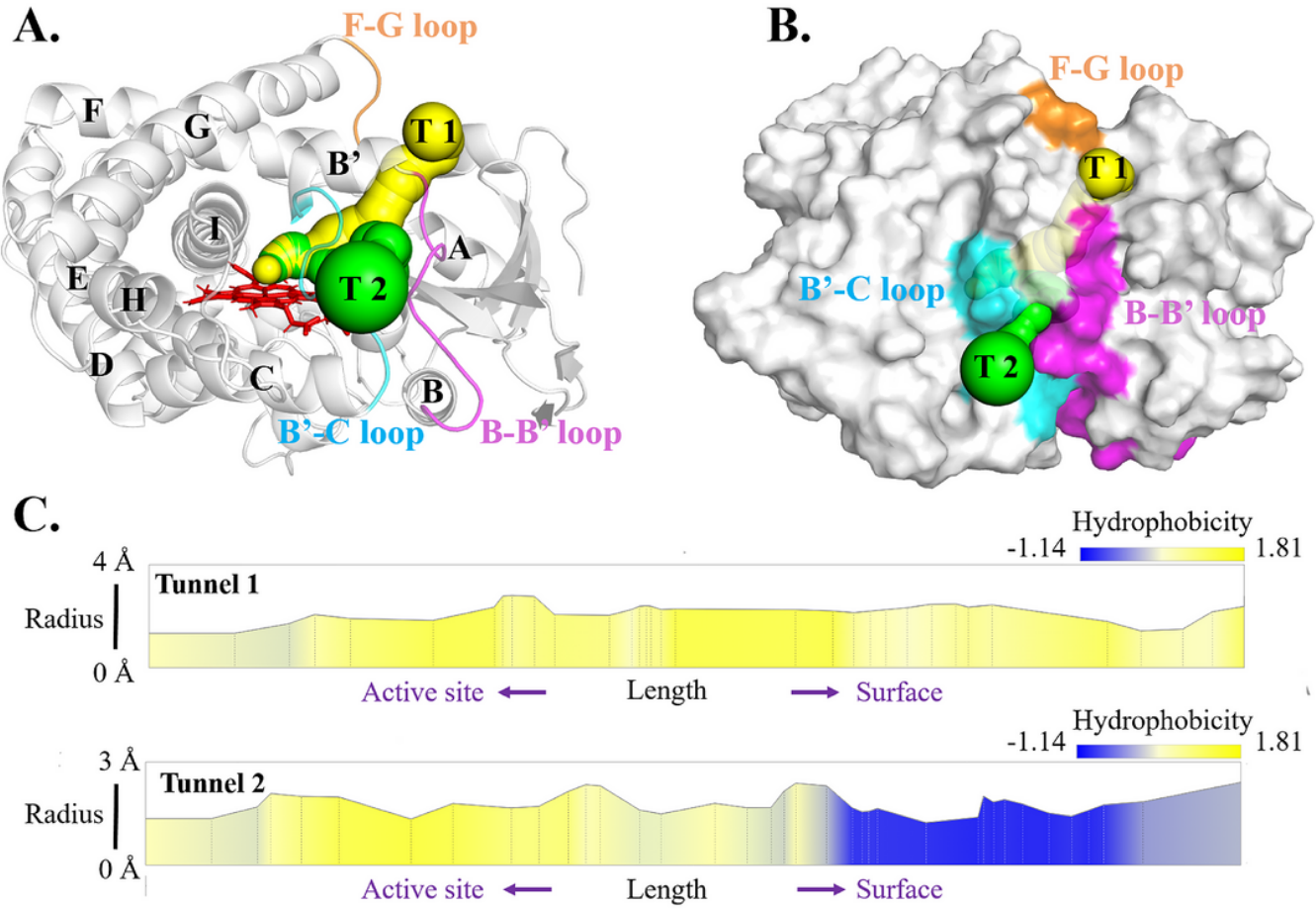

Figure 1

The overall structure and substrate access tunnels information of P450BsβHI. The structure model of P450BsβHI was constructed by PyMoL based on the crystal structure of P450Bsβ (PDB: 1IZO). The access tunnel identification and hydrophobicity analysis were carried out with MOLEonline (Pravda, L, 2018). A and B : the structure of the P450BsβHI enzyme. Access tunnel 1 (T1) and 2 (T2) were colored in yellow and green, respectively. The B-B' loop, B'-C loop and F-G loop were colored in orange, purple and cyan, respectively, C. The hydrophobicity property of identified tunnels. Hydrophobicity index accord to Hilda Cid et.al from the charged residues (Glu -1.14) to nonpolar residues (Ile 1.81) (Cid, Bunster, Canales, & Gazitúa, 1992).

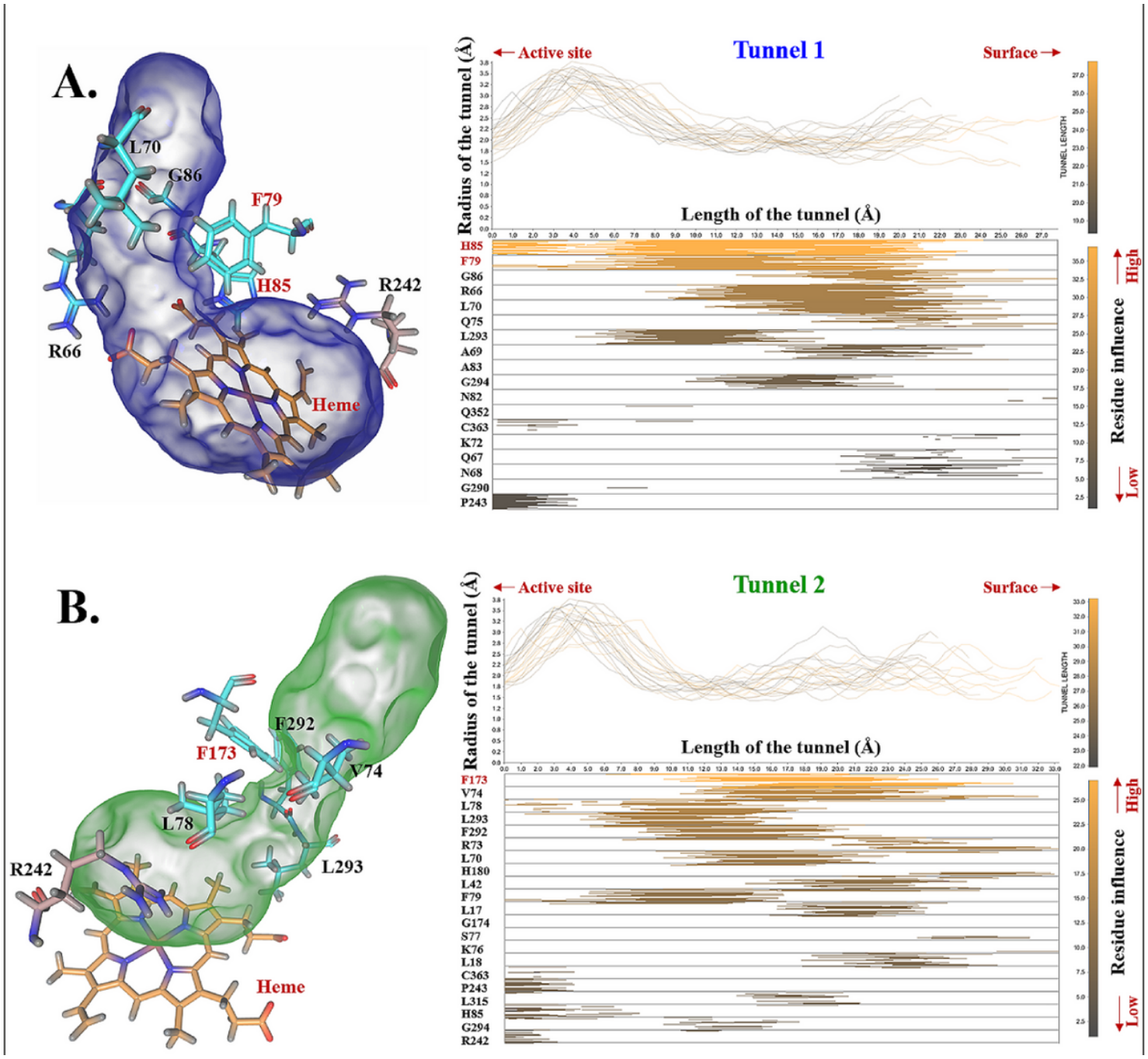

Figure 2

Evolution of residues lining the access tunnels of P450BsβHI. The access tunnel analysis was carried out with Caver Analyst 2.0 BETA. The left part is bottleneck residues lining of tunnel 1 and 2. The upper right part shows graph representation plots the tunnel width along its centerline. Each line represents the tunnel in one timestep. The lower right part describes the list of all residues contributing to the tunnel. The horizontal position of the color in the line shows which part of the tunnel this residue influences. All tunnel structure information was from the 5 ns snapshot of MD simulation.

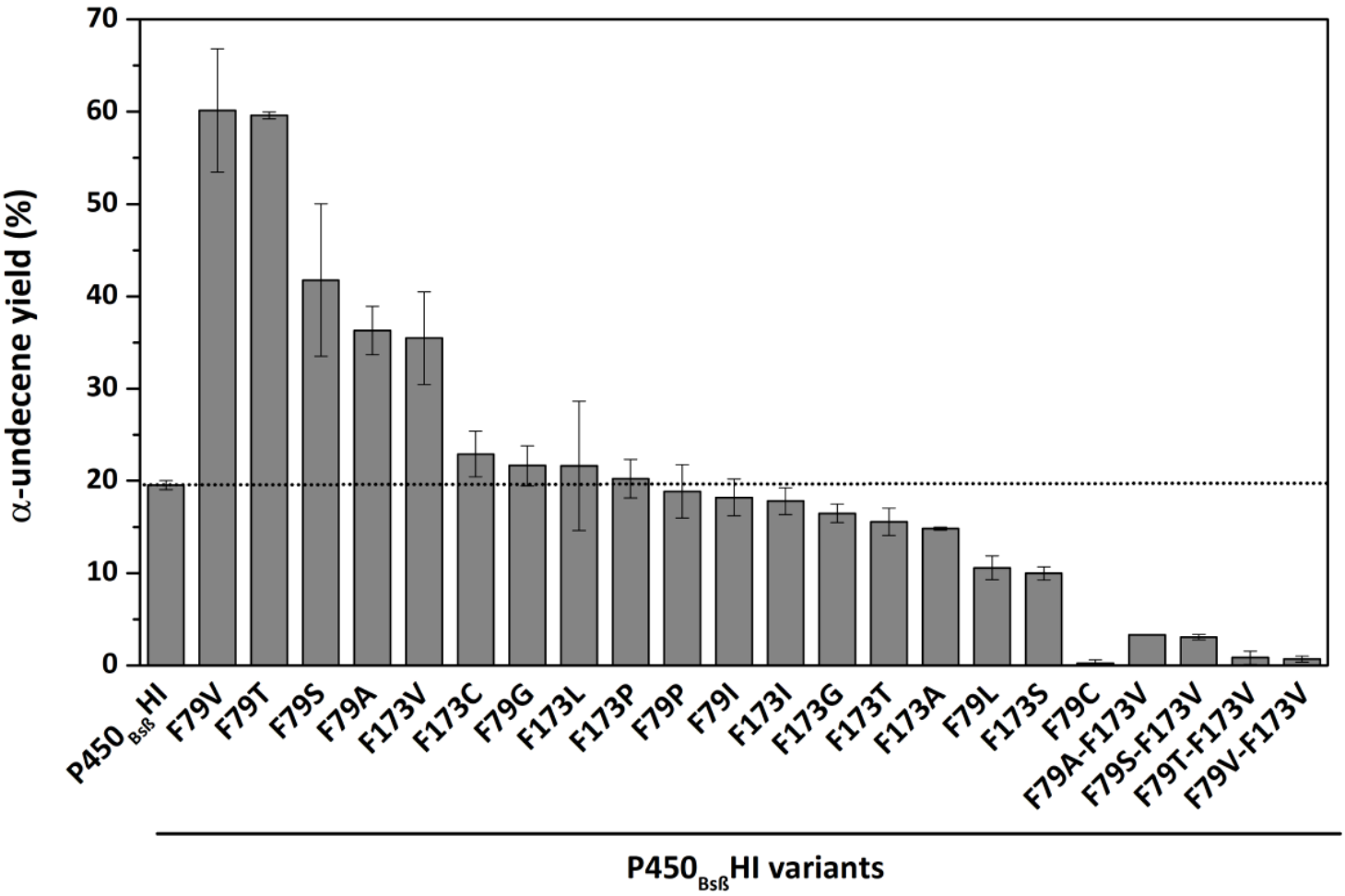

Figure 3

Evolution of the activity of P450BsβHI variants towards the decarboxylation of lauric acid. The α-undecene products were qualitatively determined by contrasting with standard sample, and quantified by external standard method. Results shown are mean ± SD of duplicated experiments.

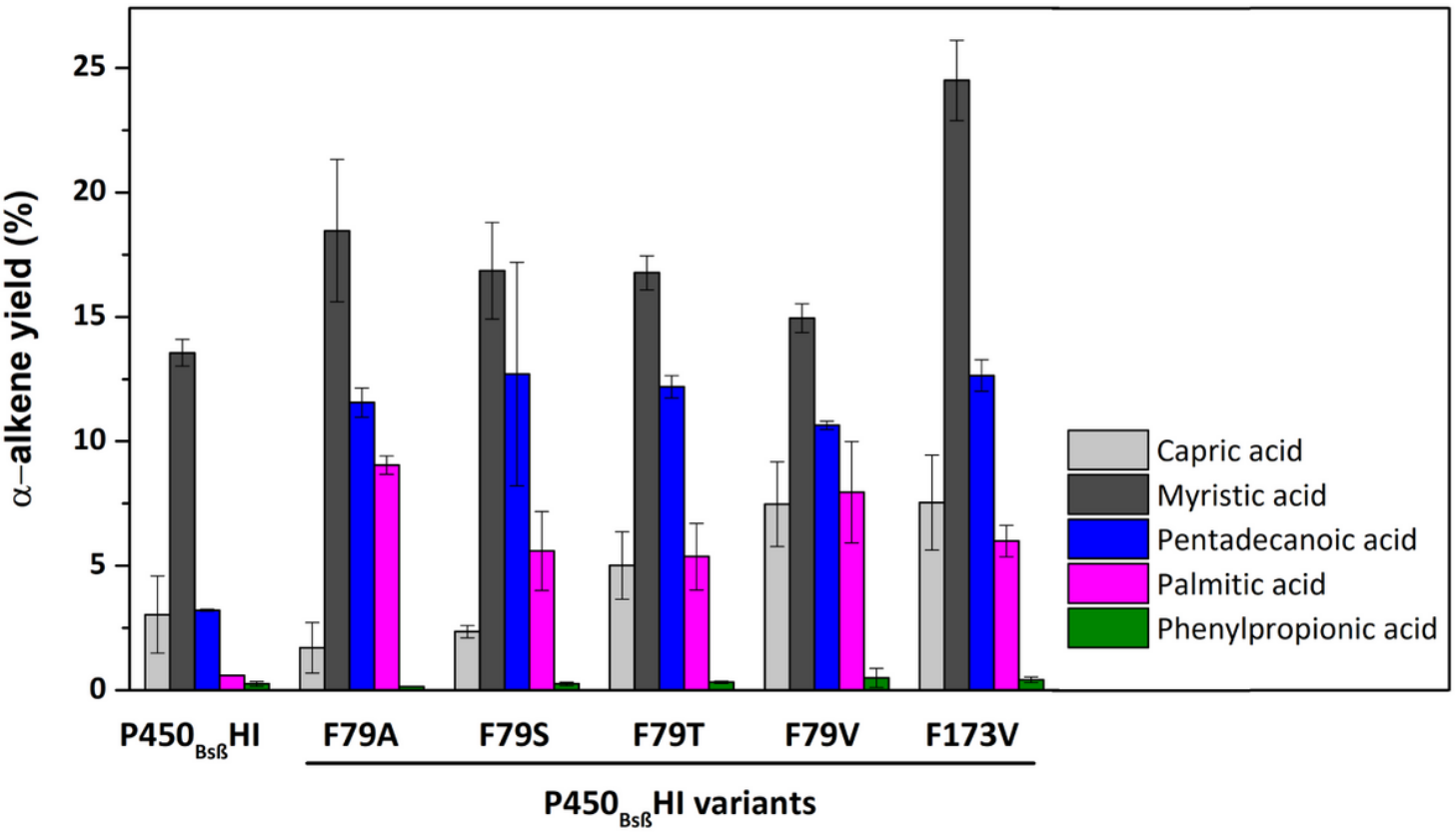

Figure 4

Decarboxylation performance of P450BsβHI and its variants towards various organic acid. Capric acid, myristic acid, pentadecanoic acid, palmitic acid, and phenylpropionic acid were used as substrate. All of the α-alkene products were qualitatively determined by contrasting with standard sample, and quantified by external standard method. Results shown are mean ± SD of duplicated experiments.

Supplementary Files

This is a list of supplementary files associated with this preprint. Click to download.

- Graphicabstract.tiff
- Supportinformation.docx